

**Journal of Superconductivity manuscript No.**  
 (will be inserted by the editor)

N. Pompeo · S. Sarti · R. Marcon · H.  
 Schneidewind · E. Silva

## Vortex state microwave resistivity in Tl-2212 thin films.

Received: date / Accepted: date

**Abstract** We present measurements of the field induced changes in the 47 GHz complex resistivity,  $\Delta\tilde{\rho}(H, T)$ , in  $\text{Tl}_2\text{Ba}_2\text{CaCu}_2\text{O}_{8+x}$  (TBCCO) thin films with  $T_c \simeq 105$  K, prepared on  $\text{CeO}_2$  buffered sapphire substrates. At low fields ( $\mu_0 H < 10$  mT) a very small irreversible feature is present, suggesting a little role of intergranular phenomena. Above that level  $\Delta\tilde{\rho}(H, T)$  exhibits a superlinear dependence with the field, as opposed to the expected (at high frequencies) quasilinear behaviour. We observe a crossover between predominantly imaginary to predominantly real (dissipative) response with increasing temperature and/or field. In addition, we find the clear scaling property  $\Delta\tilde{\rho}(H, T) = \Delta\tilde{\rho}[H/H^*(T)]$ , where the scaling field  $H^*(T)$  maps closely the melting field measured in single crystals. We discuss our microwave results in terms of loss of flux lines rigidity.

**Keywords** Tl:2212 · Microwave response · Vortex motion

### 1 Introduction

The microwave response of type-II superconductors in the vortex state is determined by a rich variety of phenomena. In principle, the response is dictated by intrinsic processes, such as the motion of Abrikosov flux lines, described by the vortex motion complex resistivity  $\tilde{\rho}_{vm} = \rho_1 + i\rho_2$ , and charge conduction, described by the complex conductivity  $\tilde{\sigma}$ , and by many extrinsic processes, related to the granularity of real samples. Focusing for the moment on intrinsic processes, when the temperature is not too close to  $T_c$  the motion of flux lines (vortices) is thought to dominate the vortex state electrodynamic response up and beyond the microwave spectrum.

A general approach to the field, frequency and temperature dependence of the vortex motion (and its

---

N. Pompeo  
 Dipartimento di Fisica "E. Amaldi" and Unità CNISM, Università di Roma Tre, Via della Vasca Navale 84, 00146 Roma, Italy

S. Sarti  
 Dipartimento di Fisica and Unità CNISM, Università "La Sapienza", 00185 Roma, Italy

R. Marcon  
 Dipartimento di Fisica "E. Amaldi" and Unità CNISM, Università di Roma Tre, Via della Vasca Navale 84, 00146 Roma, Italy

H. Schneidewind  
 Institute for Physical High Technology Jena, P.O.B.100239, D-07702 Jena, Germany

E. Silva  
 Dipartimento di Fisica "E. Amaldi" and Unità CNISM, Università di Roma Tre, Via della Vasca Navale 84, 00146 Roma, Italy  
 Tel.: +39-06-55177205  
 Fax: +39-06-5579303  
 E-mail: silva@fis.uniroma3.it

interplay with the response of the condensate) is a formidable task, that remains to be fully developed. Even the frequency dependence of vortex motion alone is still a debated topic. Nevertheless, when flux lines can be treated as rigid rods, or as fully decoupled pancakes, it is believed that at high enough frequencies the electrodynamics is essentially dictated by single-vortex response. This is due to the very small amplitude of the oscillations induced by the alternate current at high frequencies. In high- $T_c$  superconductors (HTS) at typical microwave frequencies ( $\nu \sim 10$  GHz, where  $\nu$  is the microwave frequency) the oscillations are estimated to be well below 1 nm [1]. In the single-vortex limit, the vortex motion gives rise to a microwave response determined by the vortex viscosity  $\eta$ , which takes into account the dissipation due to superfluid/quasiparticle conversion during vortex motion [2] and is determined by the upper critical field scale, and by the vortex pinning constant  $\kappa_p$ , which takes into account the elastic response of the vortex. The depinning frequency  $\nu_p = \kappa_p/2\pi\eta$  is also introduced, and it marks the crossover between the pinning dominated (Campbell) regime at  $\nu \ll \nu_p$ , where the response is predominantly imaginary, to the viscous regime (flux flow) at  $\nu \gg \nu_p$ , where the response is predominantly real and dissipative. With just these ingredients, one has the well-known Gittleman-Rosenblum model, where the vortex motion complex resistivity is given by [3]:

$$\tilde{\rho}_{GR}(H, T) = \frac{\Phi_0 B}{\eta} \frac{1 + i \frac{\nu_p}{\nu}}{1 + \left(\frac{\nu_p}{\nu}\right)^2} \quad (1)$$

where  $\Phi_0 = 2.07 \times 10^{-15}$  Tm $^{-2}$  is the flux quantum. When creep of vortices is allowed, Coffey and Clem [4] and Brandt [5] extended the model by accounting for a periodic potential and for a relaxational Labusch parameter, respectively. The resulting vortex resistivity could be written in a very similar way as:

$$\tilde{\rho}_{CCB}(H, T) = \frac{\Phi_0 B}{\eta} \frac{1 + \epsilon \left(\frac{\nu_0}{\nu}\right)^2 + i(1 - \epsilon) \frac{\nu_0}{\nu}}{1 + \left(\frac{\nu_0}{\nu}\right)^2} \quad (2)$$

where  $\epsilon \approx e^{-\frac{U}{k_B T}}$  is the creep factor,  $k_B$  is the Boltzmann constant and  $\nu_0 \rightarrow \nu_p$  in the limit  $\epsilon \rightarrow 0$ . These simple models have been effective in the description of the frequency dependence of the microwave response in conventional superconductors [3] and in YBa<sub>2</sub>Cu<sub>3</sub>O<sub>7- $\delta$</sub>  (YBCO) [2, 6, 7], sometimes with the addition of a field-independent [8, 9] or field-dependent [10] contribution of the superfluid. It should also be mentioned that, within these models, the elastic response can originate from both pinning and elasticity of the vortex line, so that care should be taken when discussing the parameters resulting from the analysis of the data: extrinsic pinning phenomena as well as vortex line tension can be in principle probed by the electromagnetic response.

It has to be noted that a crucial role is played by the measuring frequency: by lowering the frequency below the characteristic frequency  $\nu_0$  (or  $\nu_p$ ), vortices experience large drags from their equilibrium positions and they can interact with each other and with several potential wells. In this case the nature and distribution of pinning centers becomes crucial, and the various vortex phases arising [11, 12] can have very different transport properties. The same validity of the single-vortex models can then be questioned: as an experimental example, swept-frequency measurements in YBCO have shown [13] that the microwave resistivity undergoes a crossover between a collective (glassy) behaviour to the independent vortex motion around a characteristic frequency of order of a few GHz.

Granularity is sometimes indicated as a possible dominant source for the losses in the microwave response in superconducting films. Manifestations of granularity include weak-links dephasing [14], Josephson fluxon (JF) dynamics [15] and, as recently studied, Abrikosov - Josephson fluxon (AJF) dynamics [16]. Weak-links dephasing is characterized by a very sharp increase of the dissipation at dc fields of order or less than 20 mT, accompanied by a strong hysteresis [14]. Josephson fluxon dynamics has been studied essentially in relation to nonlinear effects, due to the short JF nucleation time. In fact, it has been reported [17] that in thin YBCO films nonlinear and linear phenomena are decoupled, and that linear phenomena are related to Abrikosov fluxons while JF play a role in the nonlinear response only. If however one assumes that a dc field has the same effect as a microwave field, the qualitative properties of JF dynamics would be barely distinguishable from conventional Abrikosov fluxons dynamics, since an equation like Eq.1 would hold [15], with the noticeable difference of a small viscosity due to the insulating core. Abrikosov-Josephson fluxons nucleate along small-angle grain boundaries. The ac response is expected to saturate at fields larger than a characteristic field  $H_0$ , whose estimate spans orders of magnitude [16] in the range 0.1-10 T. The explicit expression for AJ fluxon motion ac

resistance [16] yields an initial magnetic-field increase as  $\sim \sqrt{\frac{H}{H_0}}$ , with a subsequent saturation.

Up to now, the more intense experimental effort concerning the microwave properties in the vortex state has been directed to the study of YBCO, while other HTS did not receive the same attention. In particular, little is known about TBCCO, where the microwave response has been studied essentially in connection with nonlinear properties [18] due to the potential interest for applications. Aim of this paper is to present a study of the microwave response of TBCCO in the vortex state in moderate fields. It will be shown that the measured data, even if taken at the high microwave frequency of 47.7 GHz, do not exhibit free flux flow. Instead, the data exhibit a giant reactance in the intermediate field region, indicating very small flux creep and strong elastic response for fields of order of a few kG. With increasing temperature and field, we observe a crossover toward a predominantly dissipative behaviour, with  $\rho_1 > \rho_2$ . In the crossover and dissipative regions the vortex complex resistivity undergoes a field-dependent scaling: the curves of the complex resistivity  $\tilde{\rho}_{vm}(H, T) = \tilde{\rho}_{vm}[H/H^*(T)]$ , where the temperature dependence of  $H^*(T)$  reproduces the temperature dependence of the melting field as measured in single crystals, suggesting that the crossover from the elastic to the dissipative region is driven by the loss of the vortex rigidity.

## 2 Experimental setup and samples

We measured the microwave response at high microwave frequencies at 47.7 GHz in TBCCO thin films, with a moderate magnetic field ( $\mu_0 H < 0.8$  T) applied along the *c* axis at temperatures above 59 K. The 240 nm-thick films have been grown on 2" diameter CeO<sub>2</sub> buffered R-plane sapphire substrates by conventional two - step method. The resulting films show excellent (100) orientation without any (111) components and excellent in-plane epitaxy [19]. The full-width-half-maximum of the  $\theta - 2\theta$  rocking curve is 0.4°. The film under study had  $T_c \simeq 104$  K and  $J_c = 0.5$  MAcm<sup>-2</sup> measured inductively.

We measured the magnetic field dependence of the complex resistivity at 47.7 GHz by means of a sapphire dielectric resonator operating in the TE<sub>011</sub> mode. The sapphire rod was sandwiched between the superconducting film and a copper plate. With this configuration we avoided averaging the response between two different films, at the expense of a reduced sensitivity in the absolute value of the surface impedance. Nevertheless, the sensitivity was approximately two orders of magnitude higher than with our preexisting metal cavity [20]. The detailed description of the experimental setup will be presented elsewhere [21]. We checked that the corrections for the film thickness [22] were negligible with respect to the thin-film approximation, so that (in agreement with extensive simulations [23]) the measurements yield the microwave resistivity instead of the bulk surface impedance. We measured the changes of the *Q* factor and of the resonant frequency  $f_0$  of the resonator, obtaining the changes of the complex resistivity at a fixed temperature as:  $\Delta\tilde{\rho}(H, T) = \Delta\rho_1(H, T) + i\Delta\rho_2(H, T) = Gd \left[ \left( \frac{1}{Q(H, T)} - \frac{1}{Q(0, T)} \right) - 2i\frac{f_0(H, T) - f_0(0, T)}{f_0(0, T)} \right]$ . We stress that in these measurements the variation of the effective impedance does not depend on the calibration of the resonator, but only on the geometrical factor  $G \simeq 2000$  Ω and on the film thickness  $d$ , which act as a single scale factor.

Since field-dependent measurements are involved, a short discussion of possible parasitic effects is in order. In the present configuration the microwave field probes a circular area, approximately of the size of the diameter of the sapphire rod,  $\sim 2$  mm, centered on the center of the film. The edges of the film are not exposed to the microwave field, so that our measurements do not probe vortex entry and exit induced by microwave currents. Due to the field distribution of the excited mode, the peak microwave field  $\mu_0 H_{\mu w} \sim 20$  μT is reached in an annular area of  $\sim 1$  mm diameter centered on the center of the film. Thus, for all practical purposes, the amplitude of the microwave field  $H_{\mu w} \ll H$ , so all the field effects should be regarded as coming from the dc applied field. Measurements were taken at several temperatures in the range from 60 to 95 K, resulting in reduced temperature ranges above  $T/T_c = 0.55$ . Data have been collected either in zero-field-cooled, field-cooled, and on direct and reverse field-sweeping. Only at very low signal level (corresponding to low fields) we observed a detectable hysteresis, which however affects only a small part of the overall measured impedance variation (less than 0.05 % of  $\rho_1$  in the normal state). We briefly discuss this effect in the next section, but we anticipate that it is irrelevant for the purposes of this paper. As a matter of fact, we found that in the entire temperature range explored the complex response was reversible within our sensitivity for fields above 10 mT.

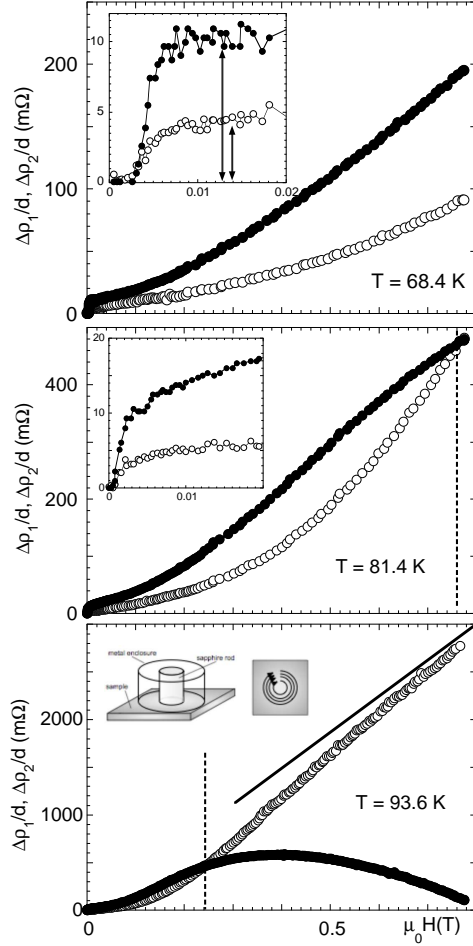


**Fig. 1** Typical measurements of the field induced change of the complex resistivity  $\Delta\tilde{\rho}$  at 47.7 GHz at various temperatures. Note the very different vertical scales of the panels. For comparison,  $\rho_1/d \approx 10 \Omega$  above  $T_c$ . Open circles: real part  $\Delta\rho_1/d$ . Full dots: imaginary part  $\Delta\rho_2/d$ . Vertical dashed lines mark the crossover field from elastic ( $\Delta\rho_2 > \Delta\rho_1$ ) to dissipative ( $\Delta\rho_1 > \Delta\rho_2$ ) response with increasing temperature and field. Continuous line in the lower panel indicates a  $\propto H$  law, typical of flux flow or rigid pinning. As can be seen, even at 93.6 K these regime are not achieved. Upper and mid insets: low field typical step-like variation of the complex resistivity, ascribed to weak links related phenomena. Lower panel inset: sketch of the experimental configuration and of the pattern of microwave currents on the sample.

### 3 Experimental results

We focus here on the data taken on one particular TBCCO sample, as representative of the behavior observed in different films prepared as described in Sec.2.

Figure 1 shows typical data for the complex resistivity shift at low, intermediate and high temperatures.

First, let us briefly discuss the low field behaviour. From the data shown in the insets of Fig. 1, it is seen that a small feature (note the expanded vertical scale, and compare to the scales for measurements at higher  $T$ ) is present below 10 mT. This feature is hysteretic, in both real and imaginary part, at low temperatures (below 70 K) and reversible above, with the hysteresis (when present) depending on magnetic history. This behaviour and the saturating field dependence after the initial steep increase are strongly reminiscent of the response of a network of weak links, due to e.g. granularity of the film under study. The distinction between all the mechanisms involved in presence of weak links [14, 15, 16] is not within the purposes of the present paper. However, as an indication for future work, it is interesting to note that in thin TBCCO films of the same origin as ours a nonlinear surface resistance at 8.5 GHz has been ascribed to AJ fluxon motion, and was found to saturate at (microwave) fields as low as  $\mu_0 H_0 \sim 1$  mT [18], similar to our range of the dc fields  $\sim 1$ -10 mT at which the low field

linear response saturates. We then argue that, in our measurements, a small part of the response is probably due to JF or AJF dynamics, even if this does not appear to be the main mechanism driving the overall measured microwave response. In the following we will concentrate on the major part of the microwave response, above the plateau of the low-field signal. In particular, we will subtract this small contribution from the remaining of the curve, that we will treat in the framework of the dynamics of Abrikosov vortices. As a consequence, we will identify our measured  $\Delta\tilde{\rho}$  with  $\tilde{\rho}_{vm}$ .

Looking at Figure 1, several features can be highlighted. First, the magnetic field dependence is clearly superlinear both in  $\Delta\rho_1$  and  $\Delta\rho_2$  in a wide range of temperatures, showing no  $\tilde{\rho} \propto H$ . Second, while  $\Delta\rho_1$  keeps increasing at all temperatures and fields, by approaching  $T_c$   $\Delta\rho_2$  changes shape, and at a certain field begins to decrease. In particular, it is seen that the complex resistivity changes several times its behaviour: at low temperatures and fields  $\Delta\rho_1 \sim \Delta\rho_2$ ; in an intermediate region one has  $\Delta\rho_2 > \Delta\rho_1$  (elastic response); by increasing field and temperature we observe a crossover from predominantly elastic (Fig. 1, upper panel) to predominantly dissipative (Fig. 1, lower panel) behaviour, marked by the crossing point of  $\Delta\rho_1$  and  $\Delta\rho_2$ .

On qualitative grounds, several remarks can be done. A large, positive reactive response can be due to the elastic response of vortex lines. In principle, it can be due to single-vortex pinning, collective pinning, elasticity of the lattice, and also to some more exotic origins such as surface pinning [24]. The collapse of the reactive response indicates that the vortex lines no more respond to some recalling force (whatever the origin), as reasonably expected when the temperature increases sufficiently. Thus, the qualitative features seem to indicate that the changes in  $\Delta\tilde{\rho}$  are dominated by vortex motion. However, a quantitative analysis is not straightforward, as we point out in the next section.

#### 4 Discussion

First, we notice that the data are not in agreement with single, rigid vortex pinning. In this case, the field dependence of the response should depend linearly on the vortex density [3,4,5], that is one should have  $\Delta\tilde{\rho} \propto B$ , which is clearly not the case even at high temperatures (Fig.1, lower panel). One could invoke nonuniform magnetic field penetration, but this seems unlikely because (1) the area probed by the microwave field is of diameter  $\sim 2$  mm, centered on a  $10$  mm  $\times$   $10$  mm film, (2) the extremely high demagnetization factor makes vortex penetration nearly coincident with the application of the field, (3) we did not observe any difference between field-cooled, zero-field-cooled and swept-field measurements (apart the tiny effect discussed above) and (4) the nonproportionality to  $H$  extends up to high temperatures.

A starting point for the analysis of the data is the general property exemplified in Fig.2: there, we show that our data for  $\Delta\rho_1$  and  $\Delta\rho_2$  obey an experimental scaling law,  $\Delta\tilde{\rho}(H, T) = \Delta\tilde{\rho}[H/H^*(T)]$ , where the temperature dependent scaling field  $H^*(T)$  is reported in the inset. The temperature dependence of  $H^*(T)$  is compared to the temperature dependence of the melting field  $H_m(T)$  as determined by  $I - V$  measurements in Tl:2212 crystals [25].

While this is a purely empirical scaling, nevertheless the quality of the collapse is remarkable. It should be mentioned that, at low reduced fields and low temperatures, the quality deteriorates, indicating eventually a breakdown of such a simple construction. However, the scaling suggests that the dynamics is mainly governed by one field scale at intermediate and high fields, while only at low fields additional mechanisms can play a role. The overall behaviour of  $\Delta\tilde{\rho}[H/H^*(T)]$  indicates a rather sharp increase of the vortex mobility around the characteristic field  $H^*$ , as indicated by the increase of  $\Delta\rho_1(H)$ . Since the temperature dependence of the scaling field tracks the melting field, we speculate that the main features of the response are dictated by some kind of vortex transformation.

To substantiate the above suggestions and speculations, we come back to the interpretation of the data by means of Eq.2. One of the main difficulties is to get information on the role of elastic response, as given by  $\nu_p$ , and of thermal depinning, as given by  $\epsilon$  and  $\nu_0$ . It is useful to introduce the ratio  $r$  defined in terms of measured quantities and related to theoretical parameters as:

$$r = \frac{\Delta\rho_2}{\Delta\rho_1} = \frac{\nu_0}{\nu} \frac{1 - \epsilon}{1 + \left(\frac{\nu_0}{\nu}\right)^2 \epsilon} \quad (3)$$

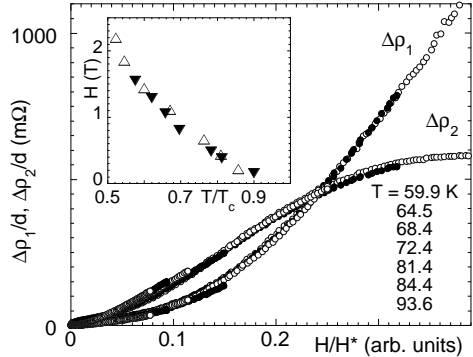


**Fig. 2** Field scaling of the complex resistivity  $\Delta\tilde{\rho}$ . With a temperature-dependent field, all pairs of curves collapse onto a single curve. In this case, we have subtracted the small junction-related signal from the total response. Inset: scaling field (full triangles) compared to the melting field  $H_m$  as obtained from dc  $I - V$  measurements in a TBCCO single crystal [25] (scaled by a factor 2.2, open triangles).

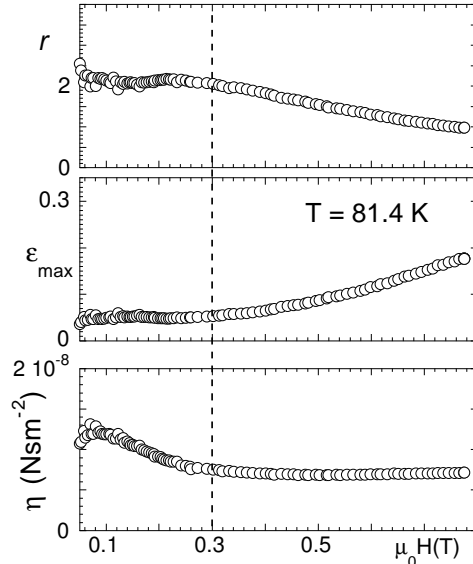


**Fig. 3** Illustration of the estimate of the maximum creep factor, the vortex viscosity and the pinning frequency at  $T = 81$  K. Upper panel: ratio  $r$  as defined in Eq.3. Above the dashed line,  $r \simeq \frac{\nu_p}{\nu}$ . Mid panel: maximum creep factor as given by Eq.4. It is seen that the maximum creep factor remains small at every field. Lower panel: calculated vortex viscosity. The procedure is selfconsistent if  $\eta$  is not field dependent. Here, for fields above 0.3 T, marked by the dashed line, the procedure yields reliable estimates of  $\eta$  and  $\nu_p$ .

With this definition, it can be shown on general grounds that, whatever the value of the characteristic frequency, one has

$$\epsilon < \epsilon_{max} = 1 + 2r^2 - 2r\sqrt{r^2 + 1} \quad (4)$$

First, we comment on the intermediate field region, where  $\Delta\rho_2 > \Delta\rho_1$ . On the basis of Eq.4, in this region  $\epsilon \ll 1$ , and  $r \simeq \frac{\nu_p}{\nu}$ . Thus,  $\eta$  can be calculated from Eq.1. To be consistent, the procedure must yield a field-independent vortex viscosity. In Fig.3 we show the result of the procedure at an intermediate temperature  $T=81.4$  K. Above  $\approx 0.3$  T we get a field independent  $\eta$ , indicating consistency of the procedure above that field. In this region, it turns out that the deviations from  $\Delta\tilde{\rho} \propto H$  have to be ascribed to a field dependence of  $k_p$ . In the same Figure we report the calculated  $r$ . In the field region where the procedure of the extraction of the vortex parameters is meaningful (i.e., where  $\eta$  is constant with the field), we observe a decrease of  $r \simeq \nu_p$  with the field, on which we will come back later.

At low  $T$  and  $H$  the calculated vortex viscosity is no more constant with the field, so that the procedure is not selfconsistent: in this case the interplay between  $\nu_0$ ,  $\nu_p$  and  $\epsilon$  in Eq.3 does not allow for a direct calculation of vortex parameters (unless multifrequency measurements can be done [7, 9, 26, 27]).

However, it is still possible to obtain some information by Eq.4, in terms of an upper bound for the creep factor. We focus momentarily on the region of moderate fields ( $0.1 \div 0.3$  T) to have an estimate of the “zero field” creep factor (upper bound) without possible artificial contributions from the small, weak-link related, anomaly. The calculation of the upper bound for  $\epsilon$  yields small  $\epsilon_{max}$  increasing from 0.015 at 60 K to 0.04 at 93.6 K. We stress again that this is only an upper bound, and nothing can be determined on, e.g., the field dependence of the true creep factor. Nevertheless, the upper bound for  $\epsilon$  gives a lower bound for the activation energies. Using  $\epsilon_{max} \approx e^{-U_{min}/k_B T}$ , we find a nearly temperature independent  $U_{min} = (18 \pm 4)$  meV (in the field region between 0.1 and 0.3 T). It is then possible to say that the potential seen by the flux lines in our TBCCO film has barriers of height that might extend down to  $\sim 20$  meV in the temperature range explored at low fields.

Now we comment on the obtained results, and we propose a general framework for our findings.

Low activation energies have been already reported in YBCO films as probed by microwave measurements [26, 27]. Remarkably, the activation energies reported in YBCO [26, 27] are compatible with the lower bound here reported for TBCCO. In both cases, the small activation energies must compare with finite critical currents and vanishing resistivity in the same field and temperature range. It is then natural to give an interpretation in terms of a very “rough” potential for flux lines, with deep wells effective for large displacements (dc currents), and many small wells which determine the effective potential barrier at high driving frequencies. As discussed by others [26, 27], such small activation energies can be taken as a manifestation of a “glassy” state, where it is not possible to push further the applicability of the CCB model, and distributions of energy barriers have to be taken into account. However, with respect to YBCO a significant difference in TBCCO appears with increasing field, indicated by the increase of vortex mobility and the drop of the imaginary part. In this case, using the CCB model a field dependent pinning frequency is obtained which is not observed in YBCO in the same field range. Even if this feature could be determined by several effects, we remark that the procedure to obtain the vortex parameters is mostly consistent in the region where the mobility increases (things that should not happen if creep effects were significant). Thus, we are led to assign the observed field dependence of the global parameter  $\nu_p$  to a field dependent  $k_p$ . The drop in  $\nu_p$  can then find an explanation in terms of loss of vortex rigidity: in the strongly anisotropic compound TBCCO, above a characteristic field the vortex can decouple or, at least, become weakly correlated along the  $c$  axis. In this case the elastic moduli decrease with the field [28], and the elastic response for small displacements becomes dominated by the “weak spring” given by the reduced elasticity of the flux line. In this frame, the scaling that we find in our data is consistent: the dynamics is dominated by the loss of rigidity, apart the low field/low temperature region. The crossover between the “mainly rigid” and “mainly uncorrelated” regimes is given by the field scale  $H^*$ , that in fact behaves as a function of the temperature as the vortex melting field [25].

While it is clear that many details still need to be worked out, the present results give an account for the complex microwave response at high driving frequencies in TBCCO in the vortex state.

## 5 Conclusion

We have presented data for the microwave resistivity in  $Tl_2Ba_2CaCu_2O_{8+x}$  thin films as a function of the temperature and magnetic field. Apart the very low fields region, where there is a possible contribution from granularity-driven processes, most of the response seems to be dominated by vortex motion. The field-dependence of the complex resistivity brings indication for strong elastic response, indicated by  $\Delta\rho_2 > \Delta\rho_1$ . We find a noteworthy scaling behaviour of the complex resistivity, where the dynamics seem to be dictated by a single field scale  $H^*(T)$ .  $H^*(T)$  reproduces the temperature dependence of the vortex melting field in TBCCO crystals, suggesting that the vortex dynamics, even at our high measuring frequencies, is dictated by some vortex transformation. The analysis by means of the Coffey-Clem-Brandt model indicates a dynamics driven by the loss of correlation of the flux lines along the  $c$  axis, as expected in layered superconductors with increasing field and temperature. We also estimate a lower bound for the activation energies for thermal depinning  $U_{min}$ . On the basis of the failure of the CCB model at low fields and temperatures, together with the low estimates for  $U_{min}$ , we suggest that at low fields the potential landscape is very rough with many low local barriers, that can give rise to a peculiar vortex dynamics, similarly to observations in YBCO. The larger anisotropy in TBCCO is suggested to be responsible for the increased mobility above a charac-

---

teristic field, above which the CCB approach is self consistent and vortex parameters can be estimated.

## References

1. W. J. Tomasch, H. A. Blackstead, S. T. Ruggiero, P. J. McGinn, J. R. Clem, K. Shen, J. W. Weber, and D. Boyne, *Phys. Rev. B*, **37**, 9864 (1988)
2. M. Golosovsky, M. Tsindlekht, D. Davidov, *Supercond. Sci. Technol.* **9**, 1 (1996), and references therein
3. J. I. Gittleman and B. Rosenblum, *Phys. Rev. Lett.* **16**, 734 (1966)
4. M.W. Coffey and J.R. Clem, *Phys. Rev. Lett.* **67**, 386 (1991)
5. E. H. Brandt, *Phys. Rev. Lett.* **67**, 2219 (1991)
6. S. Revenaz, D. E. Oates, D. Labb  -Lavigne, G. Dresselhaus, and M. S. Dresselhaus, *Phys. Rev. B* **50**, 1178 (1994)
7. S. Sarti, E. Silva, C. Amabile, R. Fastampa, M. Giura, *Physica C* **404**, 330 (2004)
8. R. Marcon, R. Fastampa, M. Giura, E. Silva, *Phys. Rev. B* **43**, 2940 (1991)
9. Y. Tsuchiya, K. Iwaya, K. Kinoshita, T. Hanaguri, H. Kitano, A. Maeda, K. Shibata, T. Nishizaki, and N. Kobayashi, *Phys. Rev. B* **63**, 184517 (2001)
10. N. Pompeo, L. Muzzi, S. Sarti, R. Marcon, R. Fastampa, M. Giura, M. Boffa, M.C. Cucolo, A.M. Cucolo, C. Camerlingo, E. Silva, *J. Phys. Chem. of Solids* **67**, 460 (2006)
11. D. S. Fisher, M. P. A. Fisher, D. A. Huse, *Phys. Rev. B* **43**, 130 (1991)
12. G. Blatter, M. V. Feigel'man, V. B. Geshkenbein, A. I. Larkin, V. M. Vinokur, *Rev. Mod. Phys.* **66**, 115 (1994)
13. D. H. Wu, J. C. Booth, and S. M. Anlage, *Phys. Rev. Lett.* **75**, 525 (1995)
14. R. Marcon, R. Fastampa, M. Giura, C. Matacotta, *Phys. Rev. B* **39**, 2796 (1989); M. Giura, R. Marcon, R. Fastampa, *Phys. Rev. B* **40**, 4437 (1989); M. Giura, R. Fastampa, R. Marcon, E. Silva, *Phys. Rev. B* **42**, 6228 (1990)
15. J. Halbritter, *J. Supercond.* **8**, 691 (1995)
16. A. Gurevich, *Phys. Rev. B* **46**, 3187 (1992); *Phys. Rev. B* **65**, 214531 (2002)
17. M.I. Tsindlekht, E.B. Sonin, M.A. Golosovsky, D. Davidov, X. Castel, M. Guilloux-Viry, A. Perrin, *Phys. Rev. B* **61**, 1596 (2000)
18. E. Gaganidze, R. Heidinger, J. Halbritter, A. Shevchun, M. Trunin, H. Schneidewind, *J. Appl. Phys.* **93**, 4049 (2003)
19. H. Schneidewind, M. Manzel, G. Bruchlos, and K. Kirsch, *Supercond. Sci. Technol.* **14**, 200 (2001); H. Schneidewind, M. Zeisberger, H. Bruchlos, M. Manzel, T. Kaiser, *Institute of Physics Conf. Series* **167**, 383 (2000)
20. E. Silva, A. Lezzerini, M. Lanucara, S. Sarti and R. Marcon, *Meas. Sci. Technol.* **9**, 275 (1998)
21. N. Pompeo, R. Marcon, E. Silva, submitted to *J. Supercond.* (2006)
22. S. Sridhar, *J. Appl. Phys.* **63**, 159 (1988)
23. E. Silva, M. Lanucara, R. Marcon, *Supercond. Sci. Technol.* **9**, 934 (1996)
24. B. Placais, P. Mathieu, Y. Simon, E. B. Sonin and K. B. Traito, *Phys. Rev. B* **54**, 13083 (1996)
25. L. Ammor, J. C. Soret, A. Smina, V. Ta Phuoc, A. Ruyter, A. Wahl, B. Martinie, J. Lecomte and Ch. Simon, *Physica C* **282** 1983, (1997)
26. N. Belk, D. E. Oates, D. A. Feld, G. Dresselhaus, and M. S. Dresselhaus, *Phys. Rev. B* **53**, 3459 (1996)
27. J. R. Powell, A. Porch, R. G. Humphreys, F. Wellh  fer, M. J. Lancaster, C. E. Gough, *Phys. Rev. B* **57**, 5474 (1998)
28. A. E. Koshelev and P. H. Kes, *Phys. Rev. B* **48**, 6539 (1993)